Asphaltene Adsorption onto Alumina Nanoparticles: Kinetics and Thermodynamic Studies

ARTICLE *in* ENERGY & FUELS · JULY 2010

Impact Factor: 2.79 · DOI: 10.1021/ef100458g

1 AUTHOR:

Nashaat N Nassar
The University of Calgary
65 PUBLICATIONS **887** CITATIONS

SEE PROFILE

Energy Fuels **2010,** *24,* 4116–4122 · DOI:10.1021/ef100458g
Published on Web 07/23/2010

energy&fuels
article

Asphaltene Adsorption onto Alumina Nanoparticles: Kinetics and Thermodynamic Studies

Nashaat N. Nassar*

Department of Chemical and Petroleum Engineering, Alberta Ingenuity Centre for In Situ Energy (AICISE), University of Calgary, Calgary, Alberta T2N 1N4, Canada

Received April 12, 2010. Revised Manuscript Received June 3, 2010

Asphaltene adsorption onto nanoparticles is an attractive subject for the heavy oil industry for two important reasons. First, nanoparticles would remove asphaltenes from the heavy oil rapidly and thus making the remaining fraction of oil transportable for conventional processing. Second, nanoparticles could be employed as catalysts for upgrading asphaltenes into light usable distillates. The first part has been investigated in this study, while the second part will be communicated shortly. In this study, the adsorption of asphaltenes from heavy oil model solutions onto colloidal nanoparticles of γ-Al_2O_3 is investigated. Batch adsorption experiments were carried out at different initial asphaltene concentrations and temperatures. The effects of the following variables on the amount of asphaltene adsorbed have been investigated, namely, contact time, initial concentration of asphaltenes, temperature, heptane/toluene ratio (H/T), coexisting molecules, and water content. Asphaltene adsorption kinetics and isotherms were obtained. The adsorption was fast, and equilibrium was approached within 2 h. The pseudo-first-order and pseudo-second-order kinetic models were applied to the experimental data, with a better fitting to the pseudo-second-order model. The resultant isotherms are in good agreement with the Langmuir isotherm model. The thermodynamics of asphaltene adsorption onto the γ-Al_2O_3 nanoparticles indicated that the adsorption was spontaneous and exothermic in nature.

1. Introduction

Asphaltenes, which are high-molecular-weight constituents of heavy oil, are very complex and not chemically identifiable compounds.[1−5] They are defined as the fraction of crude oil, bitumen, heavy oil, or vacuum residue that is insoluble in low-molecular-weight paraffin, such as *n*-pentane or *n*-heptane, while soluble in light aromatic hydrocarbons, such as toluene, pyridine, or benzene.[6] Their composition, structure, and stability depend upon their source, their method of extraction, and the type of solvent used for extraction.[2,5,7] The generic structure of asphaltenes is based on polyaromatic nuclei carrying aliphatic chains containing heteroatoms, such as nitrogen, oxygen, sulfur, and metals, such as vanadium, iron, and nickel, with an average aromatic sheet comprising 4−10 benzene-condensed rings forming monomers with an average sheet dimension in the range of 1.1−1.7 nm.[6,7] Molecular solutions of asphaltene monomers exist only for concentrations below 1 mg/L.[8] Because of intermolecular aromatic plane stacking arising from multiple interactions, these monomers become involved in networking and undergo self-association.[8−11] The most stable species are asphaltene dimers (two monomers), which are predominant at a concentration range of 5−15 mg/L. At a concentration of nearly 90 mg/L, stable quasi-spherical "nanocrystallite" dimer pairs with diameters of about 2 nm are predominant. Aggregates, which are assemblies of crystallites having an average of eight molecular stackings, form at higher concentrations.[8,9] Their sizes range between 2 and 5 nm and can associate further to form large aggregates with a diameter of 10−30 nm.[10] There is a significant effect of shear rate, asphaltene concentration, and solvent type and composition, as well as temperature and pressure, on asphaltene colloidal behavior, including shape, structure and compactness, and aggregation number.[12] There is no single value that presents asphaltene molar mass.[2] Reported molar masses are dependent upon the level of self-association and, thus, increase with the asphaltene concentration and decrease with the temperature.[13] The molar mass of asphaltenes is reported to be in the range of 750−5000 g/mol.[14] The rheological characteristics of asphaltene solutions are strongly dependent upon the molecular structure, colloidal status, and

*To whom correspondence should be addressed. Telephone: +1-403-210-9772. Fax: +1-403-210-3973. E-mail: nassar@ucalgary.ca.

(1) Toulhoat, H.; Prayer, C.; Rouquet, G. *Colloids Surf., A* **1994**, *91*, 267–283.
(2) Strausz, O. P.; Peng, P.; Murgich, J. *Energy Fuels* **2002**, *16*, 809–822.
(3) Abdallah, W. A.; Taylor, S. D. *Nucl. Instrum. Methods Phys. Res., Sect. B* **2007**, *258*, 213–217.
(4) Marczewski, A. W.; Szymula, M. *Colloids Surf., A* **2002**, *208*, 259–266.
(5) Marlow, B. J.; Sresty, G. C.; Hughes, R. D.; Mahajan, O. P. *Colloids Surf.* **1987**, *24*, 283–297.
(6) Bouhadda, Y.; Bormann, D.; Sheu, E.; Bendedouch, D.; Krallafa, A.; Daaou, M. *Fuel* **2007**, *86*, 1855–1864.
(7) Groenzin, H.; Mullins, O. C. *Energy Fuels* **2000**, *14*, 677–684.
(8) Evdokimov, I. N.; Eliseev, N. Y.; Akhmetov, B. R. *J. Pet. Sci. Eng.* **2003**, *37*, 135–143.
(9) Carlos da Silva Ramos, A.; Haraguchi, L.; Notrispe, F. R.; Loh, W.; Mohamed, R. S. *J. Pet. Sci. Eng.* **2001**, *32*, 201–216.
(10) Evdokimov, I. N.; Eliseev, N. Y.; Eliseev, D. Y. *J. Pet. Sci. Eng.* **2001**, *30*, 199–211.
(11) Mousavi-Dehghani, S. A.; Riazi, M. R.; Vafaie-Sefti, M.; Mansoori, G. A. *J. Pet. Sci. Eng.* **2004**, *42*, 145–156.
(12) Szymula, M.; Marczewski, A. W. *Appl. Surf. Sci.* **2002**, *196*, 301–311.
(13) Sztukowski, D. M.; Jafari, M.; Alboudwarej, H.; Yarranton, H. W. *J. Colloid Interface Sci.* **2003**, *265*, 179–186.
(14) Rudrake, A.; Karan, K.; Horton, J. H. *J. Colloid Interface Sci.* **2009**, *332*, 22–31.

molar masses of asphaltenes.[1,9−11,15] The increase in viscosity of crude oil with an increased asphaltene content and level of self-association is well-documented in the literature.[11,15−18] Asphaltenes can be adsorbed on surfaces as colloidal aggregates of various sizes or as individual molecules by virtue of their carboxylic and phenolic weak acidic groups. Asphaltenes adsorb onto various surfaces, creating problems during heavy oil recovery and upgrading. Asphaltenes also intensively adsorbed on mineral surfaces and reservoir rocks, forming deposits, thus limiting extraction of heavy oils from reservoirs. Asphaltene adsorption and deposition on steel surfaces limit the flow of crude oil in piping systems. Asphaltene adsorption onto the catalyst surface during catalytic upgrading of heavy oil and residue causes coke formation. In addition, asphaltenes adsorbed onto catalysts cause catalyst deactivation and poisoning.[19,20] Oil spills can cause asphaltene adsorption onto soil particles, which are difficult to clean up and would cause irreversible damage, if released to the environment. Furthermore, asphaltenes are naturally occurring surfactants that stabilize undesirable emulsions of water-in-oil and create oil separation difficulties.[21,22] These problems motivated research activities on asphaltene adsorption onto various surfaces and removal from heavy oil. Surfaces employed in previous adsorption studies included (1) metallic, such as gold,[23] steel,[3] and aluminum, and metal oxide surfaces, such titanium and iron oxides,[4] (2) mineral surfaces, such as clay,[5,24−30] mica-alumino silicate,[1,31,32] silica,[33,34] montmorillonite pillared with Al_2O_3,[28] reservoir rocks[25,35] and their components, such as quartz,[36] dolomite, calcite, and kaolin,[4] soil,[12] and mineral deposits,[37] (3) carbon,[38] and (4) glass.[39,40] The majority of the previous studies focused on adsorption isotherms. Most of these studies concluded that the adsorption isotherms are of Langmuir type I, indicating that asphaltene molecules form a single layer on the solid surface.[5,26,27,30] Other researchers criticized this representation of asphaltene adsorption and proposed a multi-layer adsorption.[4,12,25,26,34] The rate of adsorption of asphaltenes was investigated as well.[27,34,41] Typical adsorption and/or desorption kinetics were reported.[1,5,28,31,34]

Nanotechnology has potential application in heavy oil recovery and upgrading. Current research focuses on *in situ* upgrading, i.e., within reservoir, and aims at producing a medium-quality, transportable, and conventionally refinable crude oil.[42] This can be potentially accomplished through searching for suitable adsorbents that can be practically fed to the reservoir or that can be formed *in situ* using a (w/o) microemulsion technique for nanoparticle formation.[43−46] These nano-adsorbents would remove the asphaltenes from heavy oil, thus making the remaining fraction of oil easier to recover and transport. The heavy fractions are collected on the solid nano-adsorbents, which can be of catalytic nature and employed to upgrade these heavy fractions into light usable distillates. It is essential to characterize the adsorption of asphaltenes onto nanoparticles, as a first step, to establish these research activities. Interest in the application of nanoparticles for heavy oil recovery and upgrading is driven by several factors, such as providing exceptionally high surface area/volume ratios and functionalizable surface areas, which are crucial for catalytic activity and adsorption rate and selectivity. Also, nanoparticles are highly mobile in porous media because they are much smaller than the relevant pore spaces, leading to effective transport. Furthermore, nanoparticles offer potential for an environmentally friendly and cost-effective approach for heavy oil recovery and upgrading because they can be prepared *in situ*, within the oil reservoir. In this work, the use of γ-Al_2O_3 nanoparticles for adsorption of asphaltenes from heavy oil model solutions is investigated. Alumina is commonly used as a catalyst or support for heavy oil upgrading.[20]

2. Materials and Methods

2.1. Materials. Commercially available aluminum oxide, γ-Al_2O_3, nanoparticles were obtained from Sigma−Aldrich. The reported particle size is < 50 nm. The nanoparticles were used without further purifications. Before any adsorption experiments were conducted, the surface area of the γ-Al_2O_3 nanoparticles was measured by a surface area and porosity analyzer (TriStar II 3020, Micromeritics Corporate, Norcross, GA). It was found that the nanoparticles have no remarkable porosity and maintain a high external surface area (39 m^2/g). Asphaltenes were prepared from an Athabasca bitumen sample belonging to Suncor Energy and Jacos. Solvents used in the precipitation and extraction of asphaltenes and maltenes from bitumen were *n*-heptane (99%, HPLC grade, Sigma-Aldrich, Oakville, Ontario,

(15) Bockrath, B. C.; LaCount, R. B.; Noceti, R. P. *Fuel* **1980**, *59*, 621–626.
(16) Rosales, S.; Machín, I.; Sánchez, M.; Rivas, G.; Ruette, F. *J. Mol. Catal. A: Chem.* **2006**, *246*, 146–153.
(17) Wargadalam, V. J.; Norinaga, K.; Iino, M. *Fuel* **2002**, *81*, 1403–1407.
(18) Sheu, E. Y.; Shields, M. B.; Storm, D. A. *Fuel* **1994**, *73*, 1766–1771.
(19) Mochida, I.; Xing Zhe, Z.; Sakanishi, K. *Fuel* **1988**, *67*, 1101–1105.
(20) Melo Faus, F.; Grange, P.; Delmon, B. *Appl. Catal.* **1984**, *11*, 281–293.
(21) McLean, J. D.; Kilpatrick, P. K. *J. Colloid Interface Sci.* **1997**, *196*, 23–34.
(22) McLean, J. D.; Kilpatrick, P. K. *J. Colloid Interface Sci.* **1997**, *189*, 242–253.
(23) Ekholm, P.; Blomberg, E.; Claesson, P.; Auflem, I. H.; Sjöblom, J.; Kornfeldt, A. *J. Colloid Interface Sci.* **2002**, *247*, 342–350.
(24) Menon, V. B.; Wasan, D. T. *Colloids Surf.* **1987**, *23*, 353–362.
(25) Pernyeszi, T.; Patzkó, A.; Berkesi, O.; Dékány, I. *Colloids Surf., A* **1998**, *137*, 373–384.
(26) Saada, A.; Siffert, B.; Papirer, E. *J. Colloid Interface Sci.* **1995**, *174*, 185–190.
(27) González, G.; Moreira, M. B. C. *Colloids Surf.* **1991**, *58*, 293–302.
(28) Pernyeszi, T.; Dékány, I. *Colloids Surf., A* **2001**, *194*, 25–39.
(29) Bantignies, J.-L.; Cartier dit Moulin, C.; Dexpert, H. *J. Pet. Sci. Eng.* **1998**, *20*, 233–237.
(30) Gaboriau, H.; Saada, A. *Chemosphere* **2001**, *44*, 1633–1639.
(31) Drummond, C.; Israelachvili, J. *J. Pet. Sci. Eng.* **2004**, *45*, 61–81.
(32) Tong, Z. X.; Morrow, N. R.; Xie, X. *J. Pet. Sci. Eng.* **2003**, *39*, 351–361.
(33) Kumar, K.; Dao, E.; Mohanty, K. K. *J. Colloid Interface Sci.* **2005**, *289*, 206–217.
(34) Acevedo, S.; Ranaudo, M. A.; García, C.; Castillo, J.; Fernández, A.; Caetano, M.; Goncalvez, S. *Colloids Surf., A* **2000**, *166*, 145–152.
(35) Alkafeef, S. F.; Algharaib, M. K.; Alajmi, A. F. *J. Colloid Interface Sci.* **2006**, *298*, 13–19.
(36) González, G.; Middea, A. *Colloids Surf.* **1991**, *52*, 207–217.
(37) Cosultchi, A.; Garciafigueroa, E.; Mar, B.; GarcIa-Bórquez, A.; Lara, V. H.; Bosch, P. *Fuel* **2002**, *81*, 413–421.
(38) Sakanishi, K.; Saito, I.; Watanabe, I.; Mochida, I. *Fuel* **2004**, *83*, 1889–1893.
(39) Akhlaq, M. S.; Götze, P.; Kessel, D.; Dornow, W. *Colloids Surf., A* **1997**, *126*, 25–32.
(40) Castillo, J.; Goncalves, S.; Fernández, A.; Mujica, V. *Opt. Commun.* **1998**, *145*, 69–75.
(41) Jeribi, M.; Almir-Assad, B.; Langevin, D.; Hénaut, I.; Argillier, J. F. *J. Colloid Interface Sci.* **2002**, *256*, 268–272.
(42) Alberta Ingenuity Centre for In Situ Energy (AICISE). AICISE Fact Sheet 2010; http://www.aicise.ca/ (accessed on Jan 30, 2010).
(43) Nassar, N. N.; Husein, M. M. *Langmuir* **2007**, *23*, 13093–13103.
(44) Nassar, N. N.; Husein, M. M. *J. Colloid Interface Sci.* **2007**, *316*, 442–450.
(45) Nassar, N. N.; Husein, M. M. *Fuel Process. Technol.* **2010**, *91*, 164–168.
(46) Husein, M. M.; Patruyo, L.; Pereira-Almao, P.; Nassar, N. N. *J. Colloid Interface Sci.* **2010**, *342*, 253–260.

Canada) and toluene (analytical grade, EMD, Merck Group, Gibbstown, NJ).

2.2. Preparation of Heavy Oil Model Solutions. Asphaltenes were extracted from the bitumen sample with the addition of *n*-heptane as follows. A specified amount of the bitumen sample was mixed with *n*-heptane at a 1:40 (g/mL) ratio. Then, the mixture was sonicated in a water bath at 25 °C for 1 h and then transferred to a reflux extractor. The mixture was boiled under reflux for a period of 24 h to remove co-precipitated resins. Black precipitates formed at the bottom. The precipitated asphaltenes were collected after decanting the supernatant. Then, asphaltenes were washed with fresh *n*-heptane at a ratio 1:4 (g/mL), centrifuged at 5000 rpm for 5 min, and left to stand overnight. The asphaltenes were separated from the final solution by filtration using an 8 μm Whatman filter paper. The cake was washed with *n*-heptane several times until the color of the asphaltenes became shiny black. The resultant asphaltenes were homogenized and fined using pestle and mortar and left to dry at 25 °C in a vacuum oven until no change in mass was observed. The supernatant containing *n*-heptane and maltenes was transferred into a rotary evaporation unit for maltene recovery.

The model solutions for the batch adsorption experiments were prepared by dissolving a desired amount of the asphaltenes in toluene, unless otherwise specified. All samples were prepared from a stock solution containing 10 000 mg/L asphaltenes diluted to different concentrations by the addition of toluene. The initial concentration of asphaltene solutions used in the adsorption experiments ranged from 10 to 4000 mg/L. Model solutions of diluted bitumen and maltenes in toluene were also prepared for adsorption comparison.

2.3. Adsorption Experiments. Batch adsorption experiments were carried out at a ratio 1:10 (L/g) model heavy oil solution/mass of the nanoparticles. The vials were sealed properly to avoid loss of toluene by evaporation and shaken at 300 rpm in an incubator at a specified temperature until equilibrium was established. Then, the asphaltene-containing nanoparticles were separated via centrifugation at 5000 rpm for 30 min. The concentrations of the nanoparticles in the supernatant were evaluated using a UV−vis spectrophotometer (Nicolet Evolution 100, Thermo Instruments Canada, Inc., Mississauga, Ontario, Canada) and inductively coupled plasma-atomic emission spectroscopy (ICP-AES, IRIS Intrepid II XDL, Thermo Instruments Canada, Inc., Mississauga, Ontario, Canada). No significant UV peak of alumina was observed nor was an appreciable concentration detected, as confirmed by the ICP-AES, indicating that all of the nanoparticles were separated by centrifugation. The supernatant was analyzed for its asphaltene concentration using the UV−vis spectrophotometer. A calibration curve of UV−vis absorbance at ~400 nm versus the asphaltene concentration was established using standard model solutions with known concentrations.[4,8,12,47−54] The toluene solvent identical to that used for preparing model solution was used as a blank. The adsorption of asphaltenes onto nanoparticles was determined from the change in the concentration of asphaltenes in toluene before and after mixing with the nanoparticles. UV−vis spectra of asphaltenes in toluene were selected on the basis of the absorption linearity range, i.e., absorbance < 2.0.[49] For high concentrations of asphaltenes (> 150 mg/L), the asphaltene solutions were diluted with toluene to the desired absorbance value. The adsorbed amount of asphaltenes, q_t (mg/g), was calculated using the mass balance in eq 1

$$q_t = \frac{C_o - C_t}{m} V \quad (1)$$

where V is the sample volume (L), C_o is the initial concentration of asphaltenes in the solution (mg/L), C_t is the concentration of asphaltenes in the solution at a given time, t (mg/L), and m is the mass of the nanoparticles (g). When the system reaches equilibrium, q_e can be estimated from eq 1 by replacing C with C_e, where C_e is the equilibrium concentration.

Adsorption of bitumen and maltenes onto nanoparticles were also conducted in this study. Because of the artifact stemming from bitumen samples, gravimetric analyses were employed to determine the adsorption. Nanoparticles containing the adsorbed amount of bitumen were transferred to thermogravimetric analysis (TGA, Q600, TA Instruments, Inc., New Castle, DE). In these analyses, 10−20 mg of sample was used and γ-Al_2O_3 nanoparticles were used as a reference. The sample was heated in an alumina pan at a heating rate of 20.0 °C/min from 25 to 800 °C. In this case, the adsorbed amount was calculated from the differences in weight loss, before and after burning.

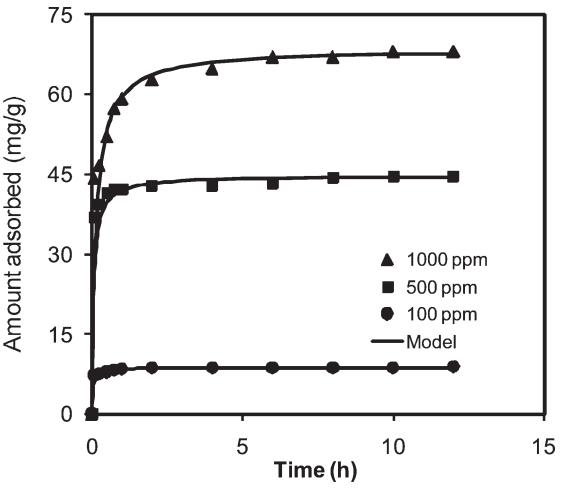

Figure 1. Amount adsorbed of asphaltenes onto γ-Al_2O_3 nanoparticles, with the change of contact time at different initial concentrations of asphaltenes. Adsorbent dose, 10 g/L; agitation speed, 300 rpm; T, 298 K. The symbols (▲, ■, and ●) are experimental data, and the solid lines are from the pseudo-second-order model (eq 5).

3. Results and Discussion

3.1. Adsorption Kinetics. The adsorption of asphaltenes onto γ-Al_2O_3 nanoparticles was monitored for 12 h at different initial concentrations of asphaltenes of 100, 500, 1000 mg/L, and the solution temperature was 25 °C. Figure 1 shows the change in the amount of asphaltene adsorbed as a function of the contact time. Evidently, asphaltenes were rapidly adsorbed onto γ-Al_2O_3 nanoparticles, and equilibrium was achieved within less than 2 h. This could be attributed to the small size of nanoparticles, which was favorable for external adsorption, where no intraparticle diffusion was observed to slow the adsorption rate. This supports the surface area measurement, which indicated that the γ-Al_2O_3 nanoparticle has no porosity. Despite the fast adsorption kinetics, a 24 h contact time was adopted as an adequate time for equilibrium to occur for the subsequent experiments. The equilibrium time is in agreement with that reported by our group for the adsorption of asphaltenes onto

(47) Al-Jabari, M. E.; Nassar, N. N.; Husein, M. M. *Proceedings of the International Congress of Chemistry and Environment* (*ICCE 2007*); Kuwait City, Kuwait, 2007.
(48) Nassar, N. N.; Al-Jabari, M. E.; Husein, M. M. *Proceedings of the 8th World Congress of Chemical Engineering* (*WCCE8*); Montreal, Quebec, Canada, 2009.
(49) Nassar, N. N.; Al-Jabari, M. E.; Husein, M. M. *Proceedings of the IASTED International Conference: Nanotechnology and Applications* (*NANA 2008*); Crete, Greece, Sept 29−Oct 1, 2008.
(50) Mozaffarian, M.; Dabir, B.; Sohrabi, M.; Rassamdana, H.; Sahimi, M. *Fuel* **1997**, *76*, 1479–1490.
(51) Goncalves, S.; Castillo, J.; Fernández, A.; Hung, J. *Fuel* **2004**, *83*, 1823–1828.
(52) Li, M. Y.; Xu, M. J.; Ma, Y.; Wu, Z. L.; Christy, A. A. *Colloids Surf., A* **2002**, *197*, 193–201.
(53) El-Sabagh, S. M. *Fuel Process. Technol.* **1998**, *57*, 65–78.
(54) Schultz, K. F.; Selucky, M. L. *Fuel* **1981**, *60*, 951–956.

Table 1. Kinetic Model Parameters for the Adsorption of Asphaltenes onto γ-Al_2O_3 Nanoparticles

		pseudo-first-order			pseudo-second-order		
initial concentration (mg/L)	q_e (experimental) (mg/g)	q_e (mg/g)	k_1 (h^{-1})	R^2	q_e (mg/g)	k_2 (h^{-1})	R^2
100	8.8	3.6	2.54	0.79	8.7	2.8	1.0
500	44.6	15.33	2.3	0.67	44.6	0.33	1.0
1000	68.0	39.6	1.66	0.81	68.5	0.1	1.0

iron oxide and nickel nanoparticles.[47,49] This is different from other conventional porous adsorbents, in which very slow asphaltene adsorption occurs through pore diffusion steps, which in turn requires a longer equilibrium time.[1,34,55]

To further investigate the kinetic mechanism that controls the adsorption process, the experimental data presented in Figure 1 were analyzed using Lagergren's pseudo-first-order model[56] and pseudo-second-order model[57] presented in eqs 2 and 3, respectively

$$\frac{dq_t}{dt} = k_1(q_e - q_t) \tag{2}$$

$$\frac{dq_t}{dt} = k_2(q_e - q_t)^2 \tag{3}$$

where q_e and q_t are the amount of asphaltenes adsorbed onto γ-Al_2O_3 nanoparticles (mg/g) at equilibrium and at any time, t (h), respectively, and k_1 and k_2 are the equilibrium rate constants of first- and second-order adsorption, respectively. Integration of eqs 2 and 3 with the boundary conditions from $t = 0$ to t and from $q_t = 0$ to q_e yields

$$\ln(q_e - q_t) = \ln(q_e) - k_1 t \tag{4}$$

$$\frac{t}{q_t} = \frac{1}{k_2 q_e^2} + \frac{t}{q_e} \tag{5}$$

When $\ln(q_e - q_t)$ versus time is plotted, one can obtain the values of k_1 from the slope and q_e from the intercept of eq 4. k_2 can be obtained by plotting t/q_t versus time. The obtained kinetic parameters are given in Table 1. It was found that the kinetic data fitted well with the pseudo-second-order adsorption model in contrast to the pseudo-first-order model, with correlation coefficient values $R^2 = 1.0$. Furthermore, the obtained theoretical values of q_e were in excellent agreement with the values obtained experimentally.

3.2. Effect of the Temperature. The effect of the temperature was investigated in the temperature range of 298−328 K. The experimental results show that adsorption of asphaltenes decreases as the temperature increases (Figure 2). This decrease in the adsorption of asphaltenes suggests that the adsorption onto the nanoparticle surface is an exothermic process. Furthermore, the temperature has an impact on the colloidal state of asphaltenes.[58,59] It is well-documented that asphaltenes may adsorb onto surfaces as colloidal aggregates, micelles, or single molecules.[31] The changes in the colloidal state of the asphaltenes can lead to a decrease in the adsorption isotherms at high temperature because of the decrease in the size of the asphaltene aggregate and asphaltene self-association.

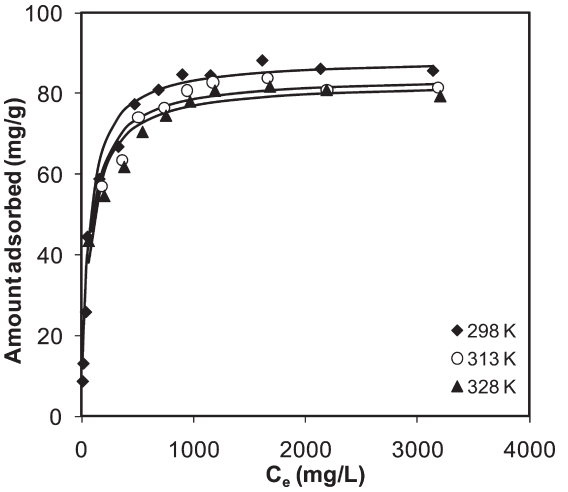

Figure 2. Adsorption isotherm of asphaltenes onto γ-Al_2O_3 nanoparticles. Adsorbent dose, 10 g/L; agitation speed, 300 rpm; T, 298 K. The symbols (◆, ○, and ▲) are experimental data, and the solid lines are from the Langmuir model (eq 6).

3.3. Adsorption Isotherms. To determine the maximum adsorption of asphaltenes and equilibrium isotherm constants, the adsorption isotherms obtained at different temperatures were further investigated (Figure 2). In all cases, Langmuir-type isotherms were observed, suggesting monolayer coverage. Similar observations have been obtained in previous studies for adsorption of asphaltenes onto clay[5,26,30] and minerals.[27] The Langmuir model assumes that adsorption occurs on a homogeneous surface by monolayer adsorption. For a gravimetric concentration, the approximated Langmuir model can be expressed by the following expression:

$$q_e = q_m \frac{K_L C_e}{1 + K_L C_e} \tag{6}$$

The linear form of the Langmuir model is given by the following equation:

$$\frac{C_e}{q_e} = \frac{1}{q_m K_L} + \frac{C_e}{q_m} \tag{7}$$

where q_e is the amount of asphaltenes adsorbed onto the nanoparticles (mg/g), C_e is the equilibrium concentration of asphaltenes in the solution phase (mg/L), K_L is the Langmuir equilibrium adsorption constant related to the affinity of binding sites (L/mg), and q_m is defined as the monolayer saturation capacity, representing the maximum amount of asphaltenes per unit mass of nanoparticles for complete monolayer coverage (mg/g). The plot of C_e/q_e versus C_e provides a straight line, as seen in Figure 3. The values of K_L and q_m were determined from the intercepts and slopes of Figure 3, respectively, and listed in Table 2. It is clear from Figure 3 and Table 2 that the experimental data fit very well to the Langmuir model. The q_m values obtained in our study are in well-agreement with those reported in the literature.[60]

(55) Kokal, S.; Tang, T.; Schramm, L.; Sayegh, S. *Colloids Surf., A* **1995**, *94*, 253–265.
(56) Ho, Y. S. *Scientometrics* **2004**, *59*, 171–177.
(57) Ho, Y. S.; McKay, G. *Process Saf. Environ. Prot.* **1998**, *76*, 332–340.
(58) Yarranton, H. W.; Alboudwarej, H.; Jakher, R. *Ind. Eng. Chem. Res.* **2000**, *39*, 2916–2924.
(59) Alboudwarej, H.; Pole, D.; Svrcek, W. Y.; Yarranton, H. W. *Ind. Eng. Chem. Res.* **2005**, *44*, 5585–5592.
(60) Dudášová, D.; Simon, S.; Hemmingsen, P. V.; Sjöblom, J. *Colloids Surf., A* **2008**, *317*, 1–9.

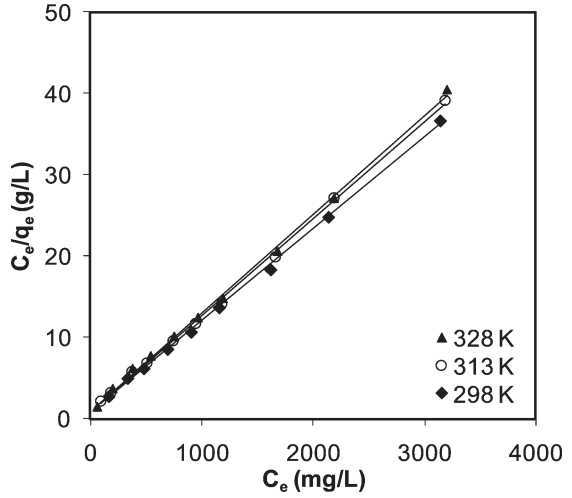

Figure 3. Linearized Langmuir isotherms of asphaltene molecules onto γ-Al_2O_3 nanoparticles at different temperatures. Adsorbent dose, 10 g/L; shaking rate, 300 rpm; contact time, 24 h.

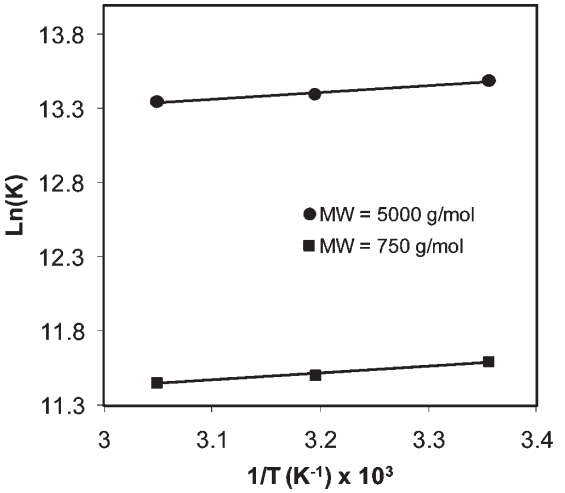

Figure 4. Estimation of thermodynamic parameters for the adsorption of different molecular masses of asphaltenes onto γ-Al_2O_3 nanoparticles.

Table 2. Estimated Parameters for the Langmuir Model at Different Temperatures

temperature (K)	q_m (mg/g)	K_L (L/mg)	R^2
298	88.5	0.015	1.0
313	84.0	0.014	1.0
328	82.6	0.013	1.0

3.4. Thermodynamic Studies. Thermodynamic studies are important for a better way of understanding the effect of the temperature on the adsorption of asphaltenes onto γ-Al_2O_3 nanoparticles. In this study, the extent of adsorption with respect to the temperature has been explained on the basis of thermodynamic parameters, such as changes in standard Gibbs free energy (ΔG^o_{ads}), enthalpy (ΔH^o_{ads}), and entropy (ΔS^o_{ads}). These parameters were determined at 298, 313, and 328 K using the Gibbs and van't Hoff equations, respectively[61]

$$\Delta G^o_{ads} = -RT \ln K \quad (8)$$

$$\ln(K) = -\frac{\Delta H^o_{ads}}{RT} + \frac{\Delta S^o_{ads}}{R} \quad (9)$$

where R is the universal ideal gas constant ($=8.314$ J mol^{-1} K^{-1}), T is the temperature (K), and K is the adsorption equilibrium constant (dimensionless). K can be expressed as $K_L C_s$, where K_L is the equilibrium Langmuir constant (L/mmol) and C_s is the solvent molar concentration (mM), which can be calculated from the density and molecular mass of toluene.[14] To determine the Langmuir constant K_L as liters per millimole, the molecular mass of asphaltenes is required. However, the asphaltene molecular mass is debatable and remains an unsolved issue, owing to the complex structure of asphaltenes.[14] Nonetheless, for the sake of having an estimate of the thermodynamic parameters of the adsorption process, the molecular mass of asphaltenes reported in the literature will be considered. Using the reported asphaltene molecular mass range of 750−5000 g/mol,[7,62] and applying the aforementioned calculations, the ΔG^o_{ads} values were found to be −33.4, −34.9, and −36.4 kJ/mol at 298, 313, and 328 K, respectively, for a molecular mass of 5000 g/mol. If the molecular mass of asphaltenes is 750 g/mol, the values of ΔG^o_{ads} were found to be −28.7, −29.9, and −31.2 kJ/mol at 298, 313, and 328 K, respectively. The negative values of ΔG^o_{ads} confirmed that the adsorption process is spontaneous and thermodynamically favorable. These values are in well-agreement to the values reported in the literature on the adsorption of asphaltenes onto metal surfaces.[14] Using the plot of the van't Hoff equation of ln(K) versus $1/T$, ΔH^o_{ads} and ΔS^o_{ads} were calculated from the slope and intercept; respectively. The van't Hoff plots are presented in Figure 4, with correlation coefficients $R^2 = 0.99$. The values of thermodynamic parameters are listed in Table 3. The negative value of ΔH^o_{ads} indicates that the interaction between asphaltenes and nanoparticles is exothermic in nature, in agreement with the finding that the adsorption is rapid and decreases with the temperature. The positive value of ΔS^o_{ads} corresponds to an increase in the randomness at the solid−liquid interface as a result of adsorption of the asphaltene molecules.

3.5. Effect of Coexisting Molecules. Maltene molecules are always present in heavy oil or bitumen, with asphaltene molecules.[5] Therefore, maltene molecules may compete with asphaltenes for the adsorption sites and interfere in the adsorption efficiency. As a result, the effect of these coexisting molecules on the asphaltene adsorption was studied at 298 K. In this set of experiments, maltenes, asphaltenes, and bitumen were redissolved independently in toluene, with the aim of obtaining an understanding on the effect of coexisting constituents on the adsorption of asphaltenes. The results are shown in Figure 5. All of the adsorption isotherms fit well to the Langmuir model. The maximum adsorption capacities and equilibrium constants are presented in Table 4. Pure asphaltenes have the highest adsorption capacity of 88.5 mg/g. The maximum adsorption capacity of bitumen is slightly lower than that of asphaltenes. On the other hand, maltenes has the lowest adsorption capacity. The differences in the adsorption can be attributed to the chemical nature and molecular size and structure of the oil constituent, which in turn affect the interaction forces between the constituent molecules and nanoparticles.[23] Nonetheless, the results suggest that asphaltene molecules have the highest interaction forces with the adsorbent surfaces. The presence of maltenes, at the considered asphaltene concentrations, can have some

(61) Smith, J. M.; VanNess, H. C.; Abbott, M. M. *Introduction to Chemical Engineering Thermodynamics*; McGraw-Hill: New York, 2005.
(62) Mullins, O. C.; Sheu, E. Y.; Hammami, A.; Marshall, A. G. *Asphaltenes, Heavy Oils, and Petroleomics*; Springer: New York, 2007.

Table 3. Calculated Values of ΔG^{o}_{ads}, ΔH^{o}_{ads}, and ΔS^{o}_{ads} for the Adsorption of Asphaltenes onto γ-Al_2O_3 Nanoparticles at Different Temperatures

asphaltene molecular mass (g/mol)	temperature (K)	K	$-\Delta G^{o}_{ads}$ (KJ/mol)	$-\Delta H^{o}_{ads}$ (KJ/mol)	ΔS^{o}_{ads} (J mol^{-1} K^{-1})	R^2
5000	298	721277	33.4	3.9	99.1	0.99
	313	659682	34.9			
	328	625442	36.4			
750	298	108192	28.7	3.9	83.3	0.99
	313	98952	29.9			
	328	93816	31.2			

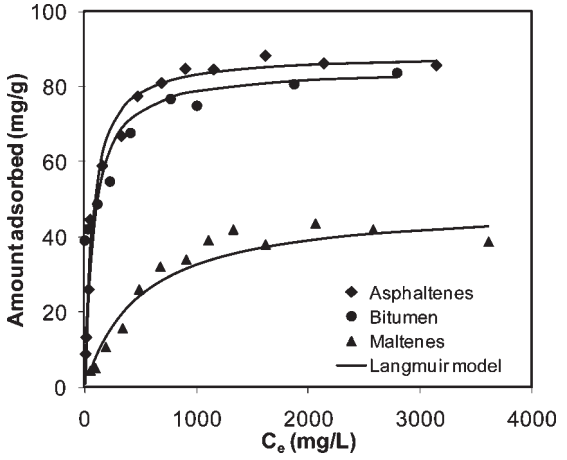

Figure 5. Effect of coexisting molecules on the adsorption of asphaltenes onto γ-Al_2O_3 nanoparticles. Adsorbent dose, 10 g/L. Points are experimental data, and solid lines are from the Langmuir model (eq 6).

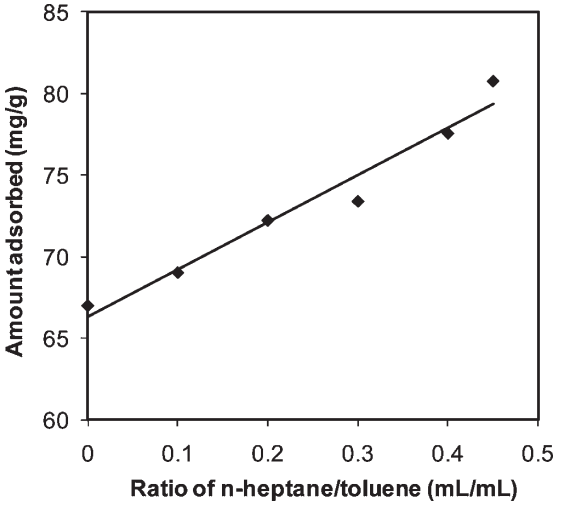

Figure 6. Effect of H/T on adsorption of asphaltenes onto γ-Al_2O_3 nanoparticles. Adsorbent dose, 10 g/L; initial concentration of asphaltenes, 1000 mg/L; agitation speed, 300 rpm; T, 298 K.

Table 4. Adsorption Capacities and Langmuir Constants of Asphaltenes, Maltenes, and Bitumen at 298 K

temperature (K)	q_m (mg/g)	K_L (L/mg)	R^2
pure asphaltenes	88.5	0.015	1.0
pure maltenes	48.5	0.002	0.96
bitumen (asphaltenes and maltenes)	84.8	0.0131	1.0

impact on this interaction because of the change in the arrangement of asphaltene molecules in the adsorbed layer as well as asphaltene aggregates. Similar observations have been reported by Marlow et al.,[5] who found that the adsorption of heavy oil constituents onto clay followed the order of pure asphaltenes > bitumen > maltenes.[5] The authors attributed these variations in the adsorption to the chemical nature and size of the adsorbate molecules and the surface area and pore size distribution of the adsorbent.

3.6. Effect of the *n*-Heptane/Toluene Ratio (H/T). It is worth mentioning that toluene is an excellent solvent for asphaltenes, while *n*-heptane is a good precipitant.[25] Thus, it is worth investigating the effect of the type of solvent on asphaltene adsorption. This was addressed by changing H/T from 0 to 0.45. A value of H/T = 0.50 was not exceeded, because increasing H/T to higher than 0.50, at fixed values of the other variables, resulted in the precipitation of asphaltenes.[59]

Figure 6 shows the amount of asphaltenes adsorbed as a function of H/T. As expected, the asphaltene adsorption increased as H/T increased. This increase can be attributed to the decrease in the solubility of asphaltenes, which, in turn, enhances asphaltene aggregation and self-association, resulting in an increase in the adsorption.[25,59]

3.7. Effect of the Water Content. Water presents at many stages during recovery, upgrading, and processing of heavy oil. Thus, it is worth investigating the effect of water on the adsorption process. In this experiment, the amount of water was increased from 0.1 to 0.25 vol % at a fixed asphaltene concentration of 1500 mg/L and temperature of 298 K. Note that the onset of phase separation occurs approximately at 0.30 vol %. Therefore, it was not possible to carry out experiments at a water content higher than 0.25 vol %. This would introduce uncertainty into the results. The amount of asphaltene adsorbed as a function of different water contents is presented in Figure 7. The figure shows that the adsorption decreased linearly as the water content increased. This can be

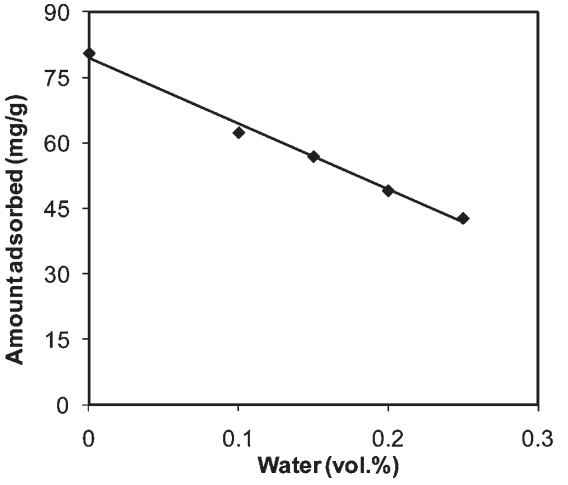

Figure 7. Effect of the water content on the adsorption of asphaltenes onto γ-Al_2O_3 nanoparticles. Adsorbent dose, 10 g/L; initial concentration of asphaltenes, 1500 mg/L; agitation speed, 300 rpm; T, 298 K.

attributed to the increase in the hydrophilicity of the adsorption surface, which drives the asphaltenes away from the accessible sites, which, in turn, decreases the adsorption.[26] Furthermore, in the presence of water, asphaltenes can act as surfactants. Accordingly, they work to stabilize water droplets within a heavy oil matrix, leading to the formation of emulsions and/or (w/o) microemulsions.[21,45] This would attract asphaltenes to the water droplets rather than nanoparticles, which again causes a decrease in the adsorption. In addition, the presence of water and emulsions can cause particle aggregation and lead to a decrease in the adsorption surface area, which impact the adsorption capacity.[45,63]

4. Conclusions

Current research trends for heavy oil upgrading focus on suitable technologies that maximize recovery and upgrading of heavy oil while minimizing the environmental footprint. This study demonstrated the use of γ-Al_2O_3 nanoparticles, as typical catalysts/supports commonly present in heavy oil upgrading, for asphaltene adsorption as a first step in *in situ* heavy oil upgrading. Asphaltene adsorption onto γ-Al_2O_3 nanoparticles was very fast, and equilibrium was achieved in less than 2 h. Kinetic study confirmed that asphaltene adsorption followed a pseudo-second-order model. Also, adsorption was highly dependent upon the initial concentration of asphaltenes, temperature, H/T, and water content. Adsorption increased as the initial concentration of asphaltenes and H/T increased. This was attributed to the increase in asphaltene self-association. On the other hand, asphaltene adsorption decreased as the water content and temperature increased. Water enhanced the hydrophilicity of the nanoparticle surface, which drives the asphaltenes away from the adsorption sites. Also, water caused particle aggregations, which impacts the adsorption capacity. Increasing the temperature caused a decrease in asphaltene self-association. The adsorption isotherms were also determined and fitted very well to the Langmuir model. Pure asphaltene has a higher adsorption capacity than bitumen or maltenes, suggesting that adsorption was affected by the chemical nature and molecular size and structure of the oil constituent. The thermodynamics of asphaltene adsorption onto γ-Al_2O_3 nanoparticles confirmed the exothermic nature and spontaneity of the adsorption process. Equilibrium constants, adsorption capacities, and thermodynamic parameters for asphaltene adsorption onto γ-Al_2O_3 nanoparticles were similar to the reported values in the literature.

Acknowledgment. The author acknowledges the funding from the Alberta Ingenuity Centre for In Situ Energy (AICISE).

(63) Husein, M. M.; Nassar, N. N. In *Microemulsions: Properties and Applications*; Fanun, M., Ed.; CRC Press, Taylor and Francis Group, LLC: Boca Raton, FL, 2009; Vol. 144; pp 465−479.